NURETH14-105

ANALISYS OF THE NUPEC PSBT TESTS WITH FLICA-OVAP PART 2: DNB BENCHMARK

Matteo Bucci and Philippe Fillion

CEA DEN/Saclay DM2S/SFME Laboratoire d'Etudes Thermohydrauliques des Réacteurs 91191 Gif sur Yvette Cedex, France matteo.bucci@cea.fr, philippe.fillion@cea.fr

Abstract

This paper discusses the results of a computational activity devoted to the prediction of boiling crisis phenomena. The capabilities of the FLICA-OVAP code have been tested against an extensive experimental database made available by the Japanese Nuclear Power Energy Corporation (NUPEC) in the frame of the PWR Subchannel and Bundle Tests (PSBT) international benchmark promoted by OECD and NRC. The experimental steady-state and transient tests herein addressed involve boiling crisis phenomena in rod bundles with uniform and non-uniform heat flux conditions. To some extent, the obtained results show good agreement between experimental data and calculations in many of the addressed conditions.

1. Introduction

Critical heat flux (CHF) is a phenomenon of great importance for reactor safety analysis and design since it defines upper limits of achievable performances in heat transfer. The understanding of this phenomenon is clearly a fundamental task, in whose aim experimental researches and computational activities have been carried out since several decades.

Computer codes must be able to predict boiling crisis phenomena, for whose validation extensive databases are required as the one available by the Japanese Nuclear Power Energy Corporation (NUPEC).

Based on NUPEC PWR Subchannel and Bundle Tests (PSBT), an international benchmark has been promoted by OECD and NRC and has been coordinated by Penn State University (PSU) [1]. The benchmark includes void distribution and departure from nucleate boiling exercises.

The Laboratoire d'Etudes Thermohydrauliques des Réacteurs (LETR) at the French Commissariat à l'Energie Atomique et aux Energies Alternatives (CEA) is involved in the PSBT benchmark performing calculations with the in-house FLICA-OVAP code [2].

FLICA-OVAP is an advanced two-phase flow thermal-hydraulics code based on a full 3D subchannel approach. It is designed to analyze flows in Light Water Reactors cores such as PWRs, BWRs and experimental reactors.

This paper is aimed at illustrating the capabilities of FLICA-OVAP in predicting boiling crisis phenomena. After a summary description of the code, a more detailed description of models available within the code to predict boiling crisis is given. Among them, two models have been applied successfully in predicting critical heat flux powers available by the NUPEC tests: the model of Shah [3] and the model of Katto and Ohno [4]. Uniform and non-uniform heat flux

conditions have been investigated in different bundle configurations representative of PWRs and BWRs assemblies. Both steady-state and transient tests have been addressed.

2. The FLICA-OVAP code

FLICA-OVAP is an advanced two-phase flow thermal-hydraulics code based on a full 3D subchannel approach, designed to analyze flows in Light Water Reactors (LWRs). It includes a Homogeneous Equilibrium Model (HEM), a four-equation drift flux model, a two-fluid model and a more general multi-field model. A detailed description of the code can be found in [5]. In this section we list the main features of the four-equation drift flux model and the relevant closure laws adopted in this analysis. The detail of the models adopted to predict boiling crisis will be also presented.

2.1 Main features of the four-equations drift-flux model

The four balance equations, describing two-phase flows in the drift flux model, are respectively the mixture mass balance equation, the mixture momentum balance equation, the mixture energy balance equation and the steam mass balance equation¹:

• mixture mass

$$\frac{\partial}{\partial t} \left(\sum_{k=n} \alpha_k \rho_k \right) + \nabla \cdot \left(\sum_{k=n} \rho_k \mathbf{u}_k \right) = 0$$

where α_k , ρ_k , \mathbf{u}_k are the volume fraction, the density and the velocity

• mixture momentum

$$\frac{\partial}{\partial t} \left(\sum_{k=v,l} \alpha_k \rho_k \mathbf{u}_k \right) + \nabla \cdot \left(\sum_{k=v,l} \alpha_k \rho_k \mathbf{u}_k \otimes \mathbf{u}_k \right) + \nabla P - \nabla \cdot \left(\sum_{k=v,l} \alpha_k \underline{\tau_k} \right) = \rho \mathbf{g} + \mathbf{F}_w$$

where P is the pressure, \mathbf{g} the gravity and \mathbf{F}_w the friction forces. The tensor $\underline{\underline{\tau}_k}$ represents the viscous and the Reynolds stress terms for the phase k. The mixture density ρ is defined as

$$\rho = \sum_{k=v,l} \alpha_k \rho_k$$

• mixture energy

$$\frac{\partial}{\partial t} \left(\sum_{k=v,l} \alpha_k \rho_k E_k \right) + \nabla \cdot \left(\sum_{k=v,l} \alpha_k \rho_k H_k \mathbf{u}_k \right) - \nabla \cdot \left(\sum_{k=v,l} \alpha_k \mathbf{q}_k \right) = q_w + \rho \mathbf{g} \cdot \mathbf{u}$$

where E_k and H_k are the total energy and the total enthalpy of the phase k, \mathbf{q}_k includes molecular and turbulent heat fluxes and q_w is the volumetric source term of thermal power.

¹ Porosities are omitted for the sake of simplicity

steam mass

$$\frac{\partial}{\partial t}(\alpha_v \rho_v) + \nabla \cdot (\alpha_v \rho_v \mathbf{u}_v) - \nabla \cdot (K_c \nabla c) = \Gamma_v$$

where c is the vapour concentration, defined as

$$c = \frac{\rho_v \alpha_v}{\rho}$$

and K_c is the corresponding diffusion coefficient. The term Γ_v represent the source terms for the vapour phase, including vapour generation on the walls or mass transfer within the bulk flow.

To estimate the relative velocity between the vapour and the liquid phase, several Zuber-Findlay type correlations are available. In this analysis the Chexal-Lellouche correlation was used [6]. Distributed pressure losses are accounted for by the product of the isothermal friction factor f_{iso} , the heating wall correction f_{heat} and the two-phase flow multiplier $f_{2\phi}$. In this analysis the Chisholm correlation [7] was used for $f_{2\phi}$, whereas the heating wall correction was estimated by an in-house model already used in the FLICA-4 code [8]. Pressure drops due to mixing or spacer

To account for turbulence effects in momentum, energy and steam mass balance equations, a turbulence model is used, permitting to estimate the different turbulent diffusivities. Moreover, the effect of grids can be accounted for by modifying certain parameters, depending whether the flow is downstream a mixing or not.

grids are instead dealt with by an anti-symmetric tensor of singular pressure drop coefficients.

Since high pressure conditions are addressed, the onset of significant void (OSV), which is the transition between single-phase heat transfer and subcooled nucleate boiling (SNB) is predicted by the Jens and Lottes correlation [9].

The mass transfer between the two phases is given by the sum of two contributions: the vapour generation on walls and the mass transfer between the liquid and the vapour phase. In subcooled nucleate boiling, only a portion of the heat flux transferred from the wall to the mixture is used to vaporize the liquid phase, whereas the remaining part is used to heat the liquid phase up.

A more detailed description of the FLICA-OVAP code can be found in [5] or [10]. In the following section, a detailed description of the models adopted to predict boiling crisis is given.

3. Prediction of the boiling crisis

To predict boiling crisis conditions, several models are currently available within FLICA-OVAP. The W3 correlation [11] is appropriate to predict departure from nucleate boiling (DNB) phenomena of interest for pressurized water reactors. However, boiling crisis experienced in NUPEC tests can be close to dryout conditions. Two models have been therefore implemented in the code: the model of Katto and Ohno [4] and the model of Shah [3]. Both models can predict critical heat flux values for both DNB and dryout conditions. An accurate description of them is given in the following sections.

3.1 The Shah model

The Shah model consists of two separate correlations to determine the *boiling number* Bo, defined as

$$Bo = \frac{q_{chf}^{"}}{G h_{lv}}$$

The first correlation covers conditions where the critical heat flux depends on the upstream conditions, named UCC (*upstream conditions correlation*). The second, named LCC (*local conditions correlation*), depends only on local quantities.

3.1.1 The UCC correlation

The UCC correlation is

Bo = 0.124
$$\left(\frac{D}{z_{eq}}\right)^{0.89} \left(\frac{10^4}{Y}\right)^n \left(1 - x_{i,eq}\right)$$

with

$$Y = \left[\frac{GDC_{p_f}}{\lambda_f}\right] \left[\frac{G^2}{\rho_f^2 gD}\right]^{0.4} \left[\frac{\mu_f}{\mu_g}\right]^{0.6}$$

In the previous equations, z_{eq} is the effective tube length and $x_{i,eq}$ is the effective inlet quality, defined as

$$x_{i,eq} = x_i$$
 $z_{eq} = z_{crit}$ for $x_i < 0$
 $x_{i,eq} = 0$ $z_{eq} = z_{sat}$ for $x_i > 0$

Where z_{crit} is the distance from the inlet section and the location of the boiling crisis, where the critical heat flux is calculated, and z_{sat} is the boiling length, which for uniformly heated tubes is given by

$$\frac{z_{sat}}{D} = \frac{z_{crit}}{D} + \frac{x_i}{4Bo}$$

For water flows, when $Y \le 10^4$, n = 0, otherwise it is given by

$$n = \left(\frac{D}{z_{eq}}\right)^{0.54} \quad \text{for } Y \le 10^6$$

$$n = \frac{0.12}{\left(1 - X_{i,eq}\right)^{0.5}} \quad \text{for } Y > 10^6$$

3.1.2 The LCC correlation

The LCC correlation is expressed by

$$Bo = F_E F_X Bo_0$$

The entrance factor F_E is given by

$$F_E = 1.54 - 0.032 \left(\frac{z_{crit}}{D}\right)$$

When the previous correlation gives $F_E < 1$, it is used $F_E = 1$.

Bo₀ is defined as the boiling number at $x_{crit} = 0$, given by the maximum value obtained by the following equations

$$\begin{aligned} \mathrm{Bo_0} &= 15 Y^{-0.612} \\ \mathrm{Bo_0} &= 0.082 Y^{-0.3} \left(1 + 1.45 P_r^{4.03} \right) \\ \mathrm{Bo_0} &= 0.0024 Y^{-0.105} \left(1 + 1.15 P_r^{3.39} \right) \end{aligned}$$

where P_r is the reduced pressure given by $P_r = P/P_c$ where P_c is the critical pressure, that is 22.064 MPa for water.

The value of F_X depends on the quality at the location of the boiling crisis x_{crit} . When $x_{crit} > 0$, the following equation is used

$$F_X = F_3 \left[1 + \frac{(F_3^{-0.29} - 1)(P_r - 0.6)}{0.35} \right]^c$$

When $P_r > 0.6$, c = 1, otherwise c = 0. F_3 is instead given by

$$F_3 = \left(\frac{1.25 \times 10^5}{Y}\right)^{0.833 \, x_{crit}}$$

When $x_{crit} < 0$, F_X is given by

$$F_X = F_1 \left[1 - \frac{(1 - F_2)(P_r - 0.6)}{0.35} \right]^b$$

As in the previous case, when $P_r > 0.6$, b = 1, otherwise b = 0. F_1 is given by

$$F_1 = 1 + 0.0052(-x_{crit}^{0.88})Y^{0.41}$$
 for $Y \le 1.4 \times 10^7$
 $F_1 = 1 + 0.0052(-x_{crit}^{0.88})(1.4 \times 10^7)^{0.41}$ for $Y > 1.4 \times 10^7$

Finally, F_2 is given by

$$F_2 = F_1^{-0.42}$$
 for $F_1 \le 4$
 $F_2 = 0.55$ for $F_1 > 4$

3.1.3 Choice between UCC and LCC correlation

For water, the UCC correlation is used when $Y \le 10^6$. When $Y > 10^6$, the correlation giving the lower value of the boiling number Bo is used, with exception of cases where $z_{eq} > 160/P_r^{1.14}$, for which the UCC formulation is always adopted. In this analysis, the UCC correlation was used in all calculations.

3.1.4 Range covered by the Shah correlation

The Shah correlation was tested against 62 experimental databases with 23 different fluids, covering the following operating conditions:

•
$$0.315 \times 10^{-3} < D < 37.5 \times 10^{-3} \text{ m}$$

The 14th International Topical Meeting on Nuclear Reactor Thermalhydraulics, NURETH-14 Toronto, Ontario, Canada, September 25-30, 2011

- 1.3 < z/D < 940
- $4 < G < 29051 \text{ kg/m}^2/\text{s}$
- $-4 < x_i < 0.85$
- $-2.6 < x_{crit} < 1$

Only 15 tests over the whole database are not included in the range covered by the Shah correlation. In the following table the values of experimental quantities relevant for the Shah model are reported.

Table 1 Range of parameters for the Shah model covered by NUPEC tests

	D [m]	z/D	G(max/min)	$x_i (max / min)$	x_{crit} (max / min)
Series 0	0.009711	376.67	4944.4 / 1408.3	-0.062 / -0.96	0.49 / -0.20
Series 2	0.009711	376.67	4769.4 / 316.7	-0.053 / - 0.97	1.00 / -0.06
Series 3	0.009989	366.21	4702.8 / 1361.1	-0.045 / - 0.87	0.58 / -0.05
Series 4	0.009711	376.67	4725.0 / 566.7	-0.058 / -0.98	1.00 / 0.06
Series 13	0.009711	376.67	3861.1 / 1361.1	-0.057 / -0.50	0.50 / 0.20
Series 8	0.008867	412.55	4816.7 / 575.0	-0.058 / -0.97	1.00 / 0.11

3.2 The Katto and Ohno model

The correlation of Katto and Ohno provides the value of the critical heat flux as

$$q_{crit}^{"} = X G \left(h_{lv} + K \Delta h_{sub.i} \right)$$

where $\Delta h_{sub,i}$ is the subcooling inlet enthalpy. The terms X and K are functions of three dimensionless terms:

$$Z' = z/D$$

$$R' = \rho_g/\rho_f$$

$$W' = \sigma \rho_f/(G^2 z)$$

Five different values of X must be determined

$$X_{1} = \frac{CW'^{0.043}}{Z'}$$

$$X_{2} = \frac{0.1R'^{0.133}W'^{0.333}}{1 + 0.0031Z'}$$

$$X_{3} = \frac{0.098R'^{0.133}W'^{0.433}Z'^{0.27}}{1 + 0.0031Z'}$$

$$X_{4} = \frac{0.0384R'^{0.6}W'^{0.173}}{1 + 0.28W'^{0.233}Z'}$$

$$X_{5} = \frac{0.234R'^{0.513}W'^{0.433}Z'^{0.27}}{1 + 0.0031Z'}$$

$$(6/18)$$

The value of C in the relationship of X_1 is given by

$$C = 0.25$$
 for $Z' < 50$
 $C = 0.25 + 0.0009(Z' - 50)$ for $50 < Z' < 150$
 $C = 0.34$ for $Z' > 150$

Three values of *K* must be determined

$$K_{1} = \frac{0.261}{CW'^{0.043}}$$

$$K_{2} = \frac{0.833[0.0124 + (1/Z')]}{R'^{0.133}W'^{0.333}}$$

$$K_{3} = \frac{1.12[1.52W'^{0.233} + (1/Z')]}{R'^{0.6}W'^{0.173}}$$

The appropriate values of *X* and *K*, must be determined according to the following Table.

Table 2 Choice of X and K for the Katto and Ohno model

Table 2 Choice of A and A to	i the ixatto and Onno model
R' < 0.15	R' > 0.15
$ \begin{cases} X_1 < X_2 & X = X_1 \\ X_1 > X_2 \\ X_2 < X_3 \end{cases} X = X_2 $	$X_1 < X_5$ $X = X_1$ $X_1 > X_5$ $X_5 > X_4$ $X = X_5$
$ \begin{pmatrix} X_1 > X_2 \\ X_2 > X_3 \end{pmatrix} X = X_3 $	$ \begin{cases} X_1 > X_5 \\ X_5 < X_4 \end{cases} $
$K_1 > K_2 K = K_1$ $K_1 < K_2 K = K_2$	$K_1 > K_2 K = K_1$ $K_1 < K_2$ $K_2 < K_3$ $K = K_2$
	$ K_1 < K_2 K_2 > K_3 $

Range covered by the Katto and Ohno correlation

The Katto and Ohno correlation covers the following operating conditions:

- 0.01 < z < 8.8 m
- 0.001 < D < 0.038 m
- 5 < Z' < 880
- 0.0003 < R' < 0.41
 3 × 10⁻⁹ < W' < 2 × 10⁻²

All experimental tests are included in the range covered by the Katto and Ohno correlation.

Table 3 Range of parameters for the Katto and Ohno models covered by NUPEC tests

	Z[m]	D [m]	Z'	R' (max/min)	W' (max / min)
Series 0	3.658	0.009711	376.67	0.159185 / 0.070185	$1.28 \times 10^{-6} / 3.97 \times 10^{-8}$
Series 2	3.658	0.009711	376.67	0.158337 / 0.030672	$5.04 \times 10^{-5} / 4.13 \times 10^{-8}$
Series 3	3.658	0.009989	366.21	0.156657 / 0.070549	$1.33 \times 10^{-6} / 4.28 \times 10^{-8}$
Series 4	3.658	0.009711	376.67	0.156156 / 0.031256	$1.35 \times 10^{-5} / 4.17 \times 10^{-8}$
Series 13	3.658	0.009711	376.67	0.156156 / 0.096048	$6.76 \times 10^{-7} / 8.28 \times 10^{-8}$
Series 8	3.658	0.008867	412.55	0.156323 / 0.031191	$1.48 \times 10^{-5} / 3.99 \times 10^{-8}$

4. Results of the computational analysis

The two models adopted in this work, the Shah and the Katto and Ohno models, have been developed and tested mostly in single channel uniform heat flux conditions [4].

In this work, the applicability of them to bundle geometries with non uniform heat flux profile has been investigated. Each experimental series of the NUPEC database has been calculated by the two models, adopting a twofold approach.

In a first step, homogenised one-dimensional calculations have been performed, adopting a bundle-averaged description.

In a second step, three dimensional calculations have been performed, adopting a subchannel description. In this case, the two boiling crisis models are applied at the sub-channels scale. The fundamental difference with the first approach consists on having different hydraulic diameters depending whether the selected sub-channel is a central, a side or a corner sub-channel. However, some special approach has to be taken for side and corner subchannels, since CHF models tend to underestimate their critical heat flux. Moreover, as observed by Tong and Tang (cfr. [12], section 5.4.5.2, Fig. 5.54), for a given inlet enthalpy, critical heat fluxes in the presence of cold walls are even higher than for internal subchannels. For the sake of simplicity, the possibility to have boiling crisis in side and corner subchannels was thus excluded.

In the following paragraphs, for each series, results obtained via the bundle-averaged and the subchannel approach will be shown for the two models. The performances of the different models are also summarized in Table 5.

4.1 Steady-state series

4.1.1 Series 0, Series 2 and Series 3

Series 0, Series 2 investigate boiling crisis in rod bundle (rods array: 5×5) and uniform heat flux. The two series differ only for the position of mixing and spacer grids. In Series 3, the bundle is also modified, adopting an array of 36 rods (6×6). The axial power shape is uniform for all series, but peripheral rods have a slightly lower power with respect to central rods: the radial power distribution factor is 0.85 for peripheral rods and 1.0 for central rods [1].

In Figure 1, Figure 2 and Figure 3, calculated and experimental critical heat fluxes are compared respectively for Series 1, Series 2 and Series 3. It is ascertained that the Shah model tends to predict higher critical heat flux values than the Katto and Ohno model, for both the bundle-averaged and the subchannel approach. Moreover, in this particular configuration with uniform heat flux and a moderate radial offset, 1D or 3D calculations give very similar results.

4.1.2 Series 4 and Series 13

Series 4 and Series 13 introduces the effect of non uniform axial profile. A cosine shape was adopted on the same bundle geometry used for Series 2. To deal with non uniform heat flux, a correction factor was adopted, as proposed by Tong [12]. In Figure 4 and Figure 5 calculated and experimental critical heat fluxes are compared respectively for Series 4, Series 13. As for previous tests, the Shah model predict higher critical heat flux values than the Katto and Ohno model, providing a better agreement with experimental values. Minor differences are experienced between the homogenized and the subchannel description.

4.1.3 Series 8

Series 8 includes the presence of a central thimble rod, representing guide tube for control rods. Contrarily to the previous series, the results of the homogenized and the subchannel approaches are different. As expected, in the presence of a radial heterogeneous power shape, a better description is achieved with the subchannel approach. In general the Shah model gives a better estimate of critical heat fluxes.

4.2 Transient Series

Two experimental campaigns have been consecrated to detect boiling crisis in transient conditions. Different transient conditions have been investigated by NUPEC, including power increase, inlet temperature decrease, flow reduction and depressurization. Two series of data have been proposed, Series 11 and Series 12, involving different bundle configurations. Series 11 is based on the bundle configuration adopted for Series 4 (cosine axial power shape, rods array 5×5), whereas Series 12 involves a central thimble rod. In the following tables, results obtained by the Shah model with the subchannel approach are listed. Boiling crisis is relatively well predicted for Series 11, whereas a larger discrepancy is ascertained for Series 12.

Table 4 Comparison between experimental and calculated boiling crisis detection time

Boiling crisis	Series11		Series 12	
detection time (s)	EXP	CALC	EXP	CALC
Power Increase	106.7	108.7	86.6	72.2
Flow Reduction	52.9	48.8	55.0	42.9
Depressurization	88.8	90.8	143.8	140.9
Temperature decrease	140.6	143.3	128.8	121.4

5. Conclusions and future perspectives

This paper has presented the current capabilities of the FLICA-OVAP code in predicting boiling crisis phenomena. The NUPEC database released in the frame of the OECD/PSBT international benchmark has been addressed. Two different models have been tested: the Shah and the Katto and Ohno model. Both a bundle averaged and subchannel approaches have been investigated. The Shah model, as implemented in the FLICA-OVAP code allows achieving a better prediction of critical heat fluxes in the different investigated configurations. Nevertheless, when the details of the radial power shape become important, better agreement was obtained with the subchannel approach permitting a local description of bundle thermal-hydraulics. Encouraging results were also obtained in the analysis of transient tests aimed at predicting the onset of boiling crisis.

Future activities are also planned for future developments of the code, including the implementation of Groeneveld's table [13] and other models based on local approaches.

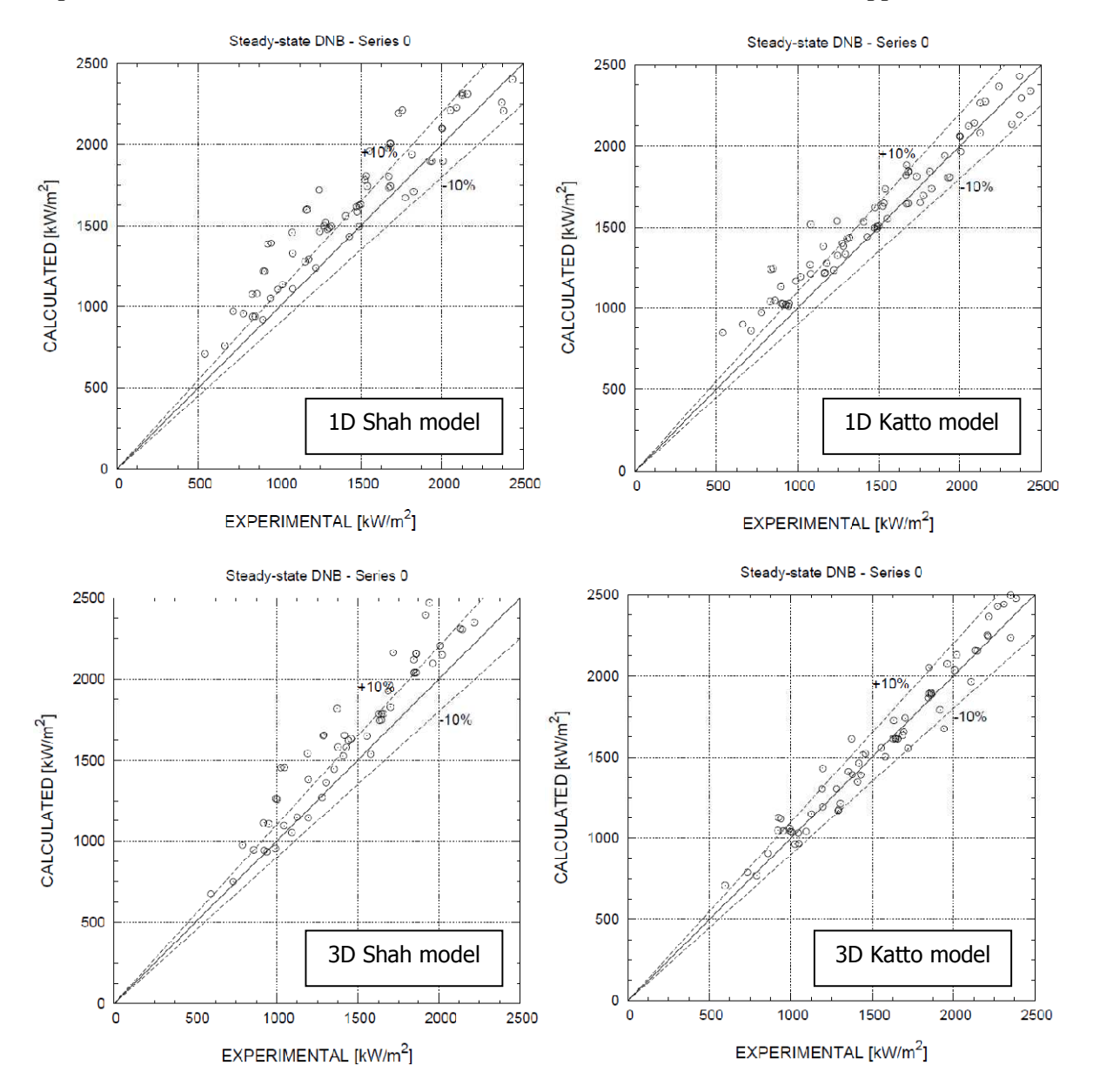


Figure 1 Computed vs. experimental critical heat fluxes (Series 0)

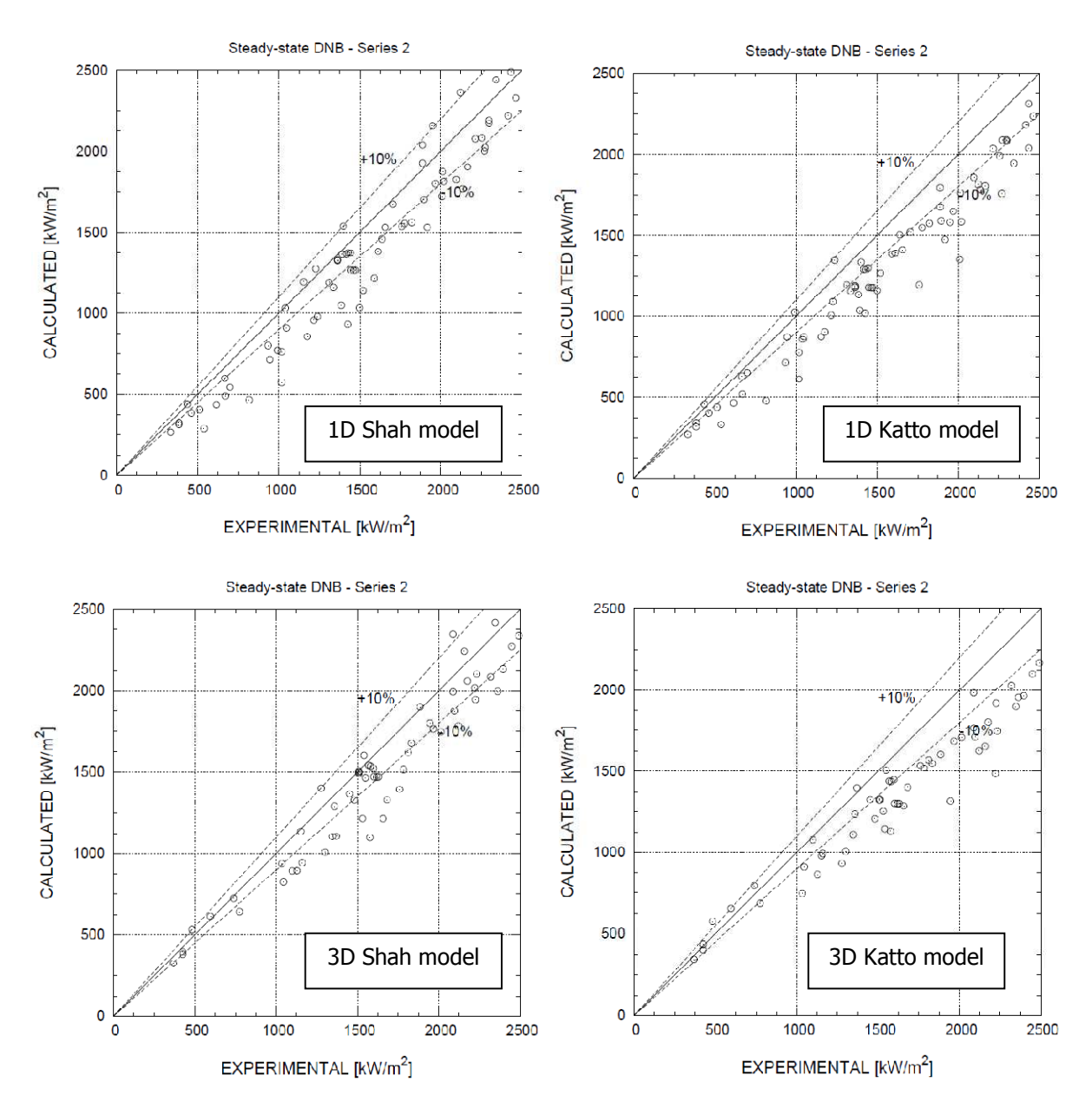


Figure 2 Computed vs. experimental critical heat fluxes (Series 2)

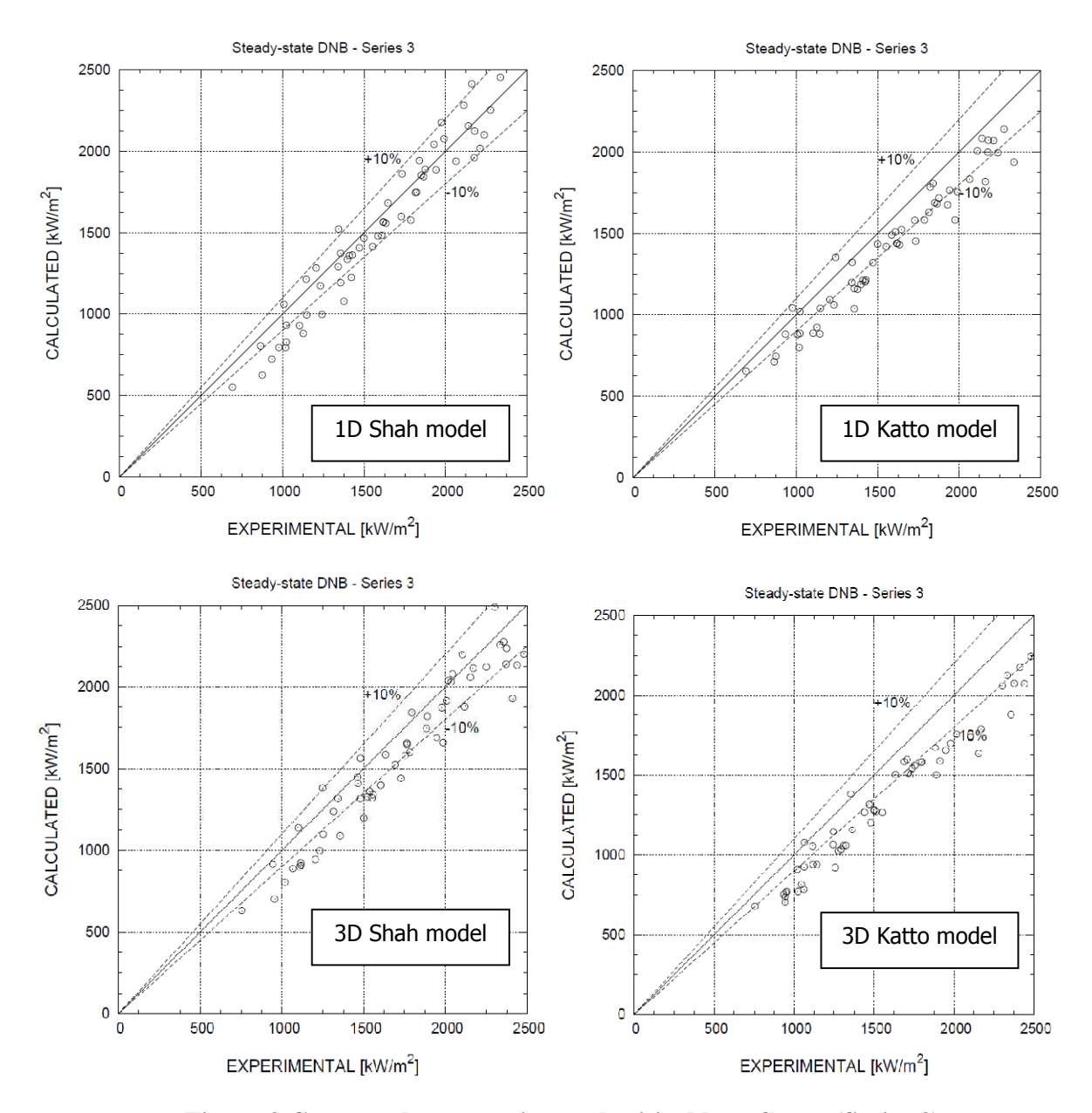


Figure 3 Computed vs. experimental critical heat fluxes (Series 3)

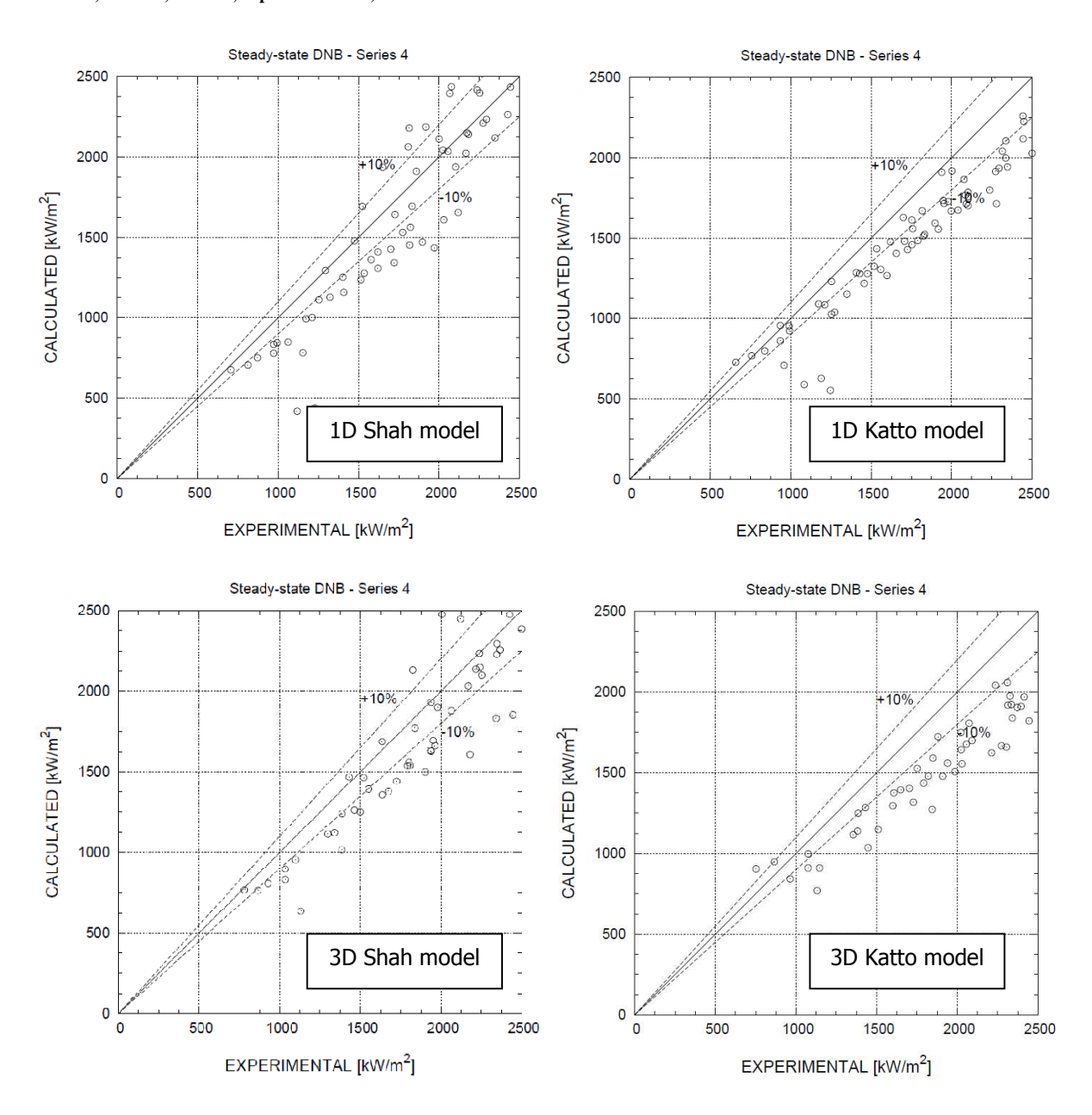


Figure 4 Computed vs. experimental critical heat fluxes (Series 4)

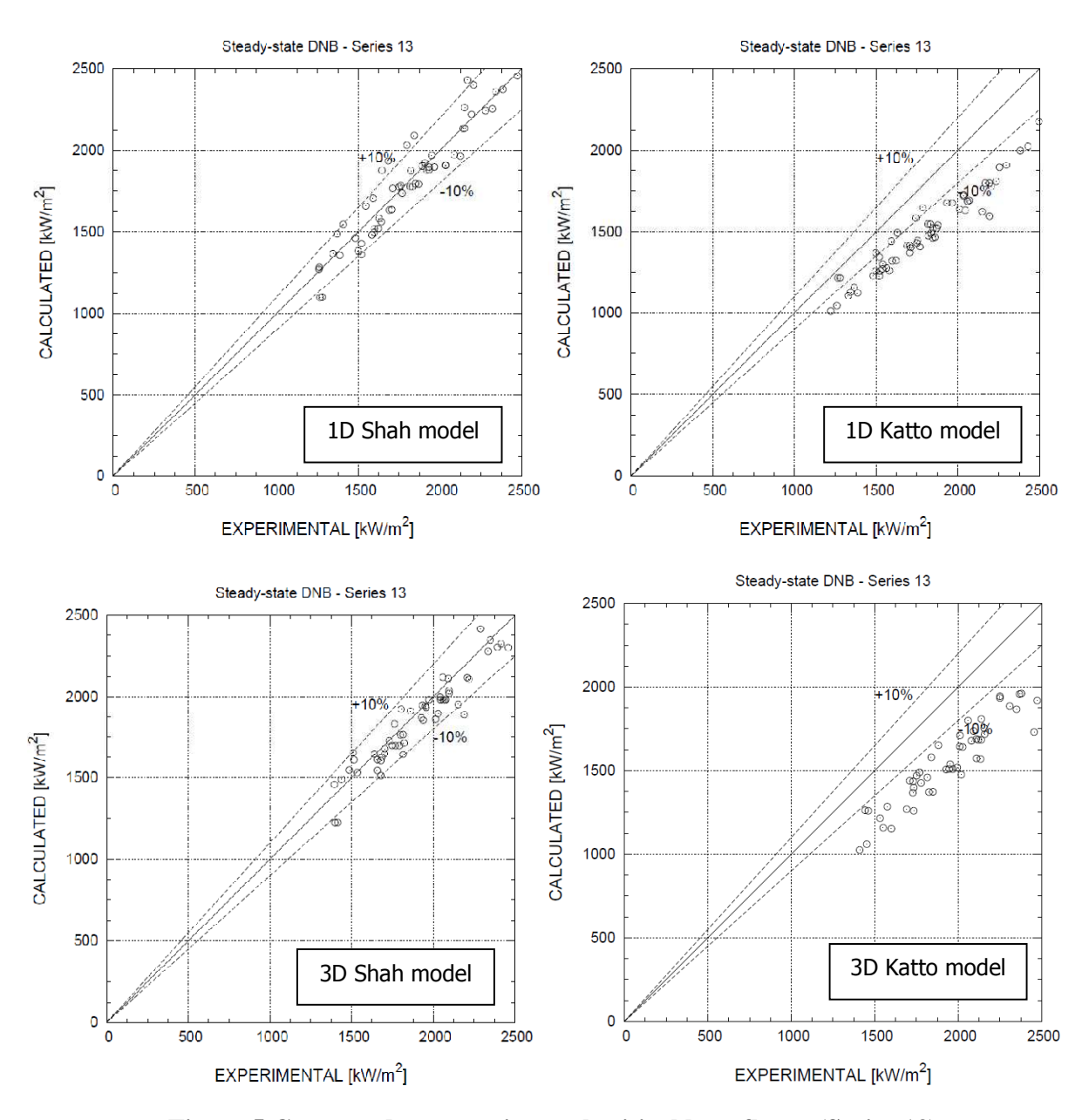


Figure 5 Computed vs. experimental critical heat fluxes (Series 13)

The $14^{\rm th}$ International Topical Meeting on Nuclear Reactor Thermalhydraulics, NURETH-14 Toronto, Ontario, Canada, September 25-30, 2011

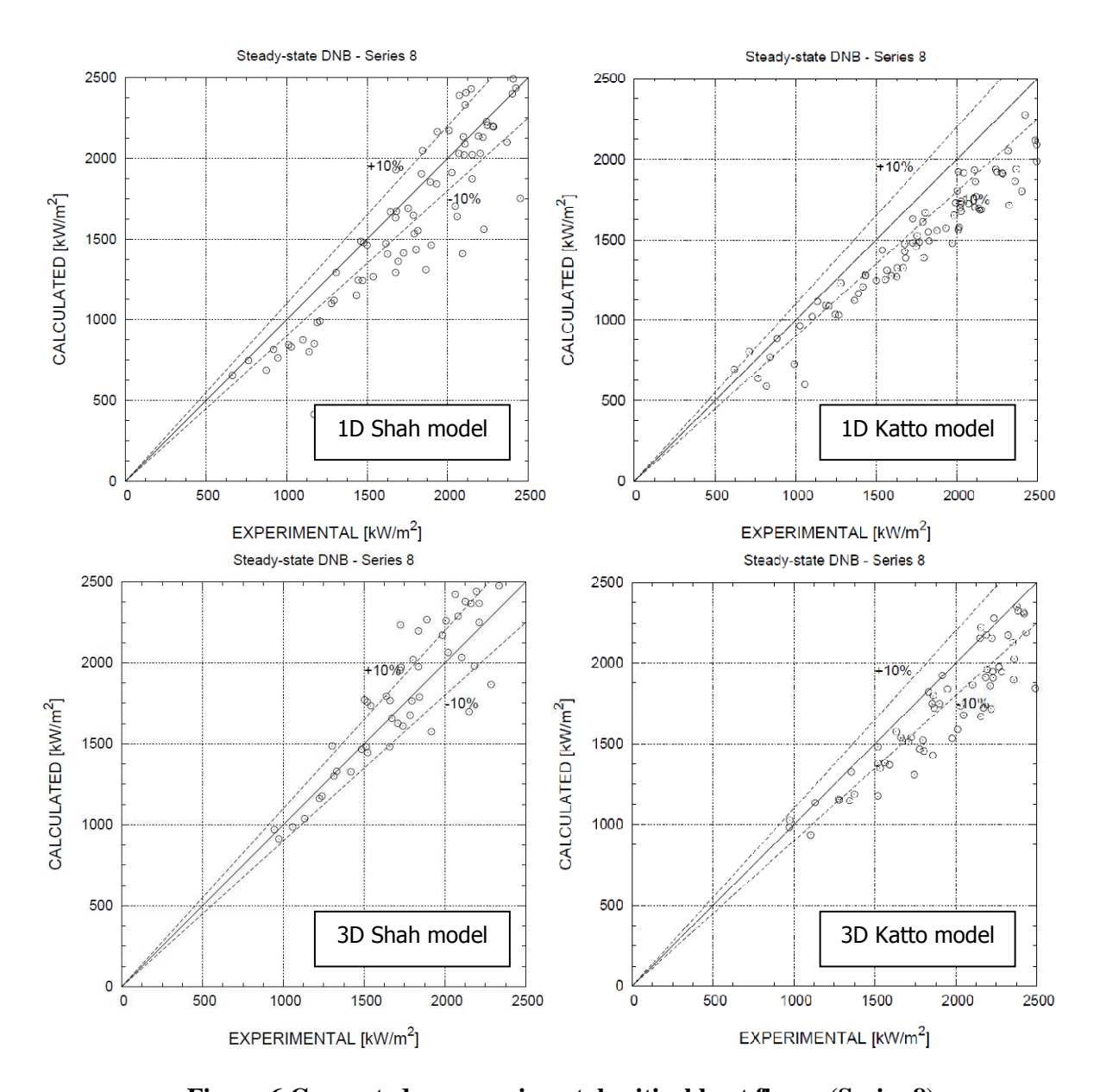


Figure 6 Computed vs. experimental critical heat fluxes (Series 8)

Table 5 Average absolute errors (%)

		- 0	\ /	
	1D Shah	1D Katto and Ohno	3D Shah	3D Katto and Ohno
Series 0	15,5	10,9	13,7	5,6
Series 2	13,5	16,0	12,3	18,3
Series 3	8,5	10,9	10,0	15,0
Series 4	14,8	14,6	13,7	19,1
Series 8	11,5	15,6	14,3	12,9
Series 13	4,8	16,4	4,6	19,6

6. Nomenclature

<u>Latin letters</u>		
Во	boiling number	[-]
Bo_0	parameter of the Shah model	[-]
С	vapor concentration	[-]
С	function of the Katto model	[-]
Cp	specific heat	[J/kg/K]
D	hydraulic diameter	[m]
E	internal energy	[J/kg]
F_E, F_X, F_1, F_2, F_3	functions of the Shah model	[-]
$\mathbf{F}_{\mathbf{w}}$	friction forces	[Pa/m]
g	gravity acceleration	$[m/s^2]$
G	mass flux	$[kg/m^2s]$
Н	enthalpy	[J/kg]
$\Delta h_{sub,i}$	subcooling inlet enthalpy	[J/kg]
h_{lv}	latent heat	[J/kg]
K_c	diffusion coefficient of steam	[kg/m/s]
K, K_1, K_2, K_3	functions of the Katto model	[-]
P	pressure	[Pa]
P_c	critical pressure	[Pa]
P_r	reduced pressure	[-]
q	heat flux	$[W/m^2]$
9 0", c	critical heat flux	$[W/m^2]$
q'' _{chf} R'	function of the Katto model	[-]
t	time	[s]
\mathcal{T}	temperature	[K]
u	velocity	[m/s]
W'	function of the Katto model	[-]
X_1, X_2, X_3, X_4, X_5	functions of the Katto model	= =
X_1, X_2, X_3, X_4, X_5	flow quality	[-] [-]
Y	function of the Shah model	[-]
_	elevation	[m]
z Z'	function of the Katto model	
L	function of the Katto model	[-]
<u>Greek letters</u>		
α	void fraction	[-]
ρ	density	$[kg/m^3]$
λ	thermal conductivity	[W/m/K]
μ	dynamic viscosity	[Kg/s/m]
σ	surface tension	[Pa.m]
T	rigaona strong tongor	$[D_{\alpha}]$

viscous stress tensor

[Pa]

<u>Subscripts</u>	
f	
g	

k

refer to saturated liquid refer to saturated vapour refer to the generic phase k

l refer to liquid refer to vapour 12

7. References

- [1] A. Rubin, A. Schoedel, M. Avramova, and H. Utsuno, "OECD/NRC benchmark based on NUPEC PWR subchannel and bundle tests (PSBT). Volume I: Experimental Database and Final Problem Specifications", Tech. Rep. NEA/NSC/DOC(2010)1, NEA/NSC, Nov. (2010).
- P. Fillion, A. Chanoine, S. Dellacherie, and A. Kumbaro, "FLICA-OVAP: a New [2] Platform for Core Thermal-hydraulic studies", in Proceedings of NURETH-13, Kanazawa, Japan, Sep. 26 – Oct. 2 (2009).
- M.M. Shah, "Improved general correlation for critical heat flux during upflow in [3] uniformly heated vertical tubes", *Heat and Fluid Flow*, **8**, no. 4, pp. 326-335, (1987).
- Y. Katto and H. Ohno, "An improved version of the generalized correlation of critical [4] heat flux for the forced convective boiling in uniformly heated vertical tubes", International Journal of Heat and Mass Transfer, 27, no. 9, pp. 1641-1648, (1984).
- M. Bucci, A. Charmeau, and P. Fillion, "FLICA-OVAP: Elements of validation for [5] LWRs thermal-hydraulic studies", in Proceedings of the ICAPP 2011, Nice, France, May 2-5 (2011).
- B. Chexal, G. Lellouche, J. Horowitz, and J. Healzer, "A Void Fraction Correlation for [6] Generalized Applications", *Progress in Nuclear Research*, 27, no. 4, pp. 255-295, (1992).
- D. Chisholm, "Friction during the flow of two-phase mixtures in smooth tubes and [7] channels", Tech. Rep. NEL-4627, National Engineering Laboratory, Department of Trade and Industry, (1972).
- E. Royer, S. Aniel, A. Bergeron, P. Fillion, D. Gallo, F. Gaudier, O. Grégoire, M. Martin, [8] E. Richebois, P. Salvatore, S. Zimmer, T. Chataing, P. Clément, and F. François, "FLICA4: Status of numerical and physical models and overview of applications", in Proceedings of NURETH-11, Avignon, France, October 2-6 (2005).
- [9] W. Jens and P. Lottes, "Analysis of heat transfer burnout, pressure drop and density data for high pressure water", Tech. Rep. ANL-4627, ANL, (1951).
- P. Fillion and M.Bucci, "Analysis of the NUPEC PSBT tests with FLICA-OVAP, part 1: [10] void distribution benchmark", in Proceedings of NURETH-14, Toronto, Canada, September 25-30 (2011).
- [11] N.E. Todreas and M.S. Kazimi, "Nuclear Systems I", Taylor & Francis, 1993.

- [12] L.S. Tong and Y.S. Tang, "Boiling heat transfer and two-phase flow", Taylor & Francis, second edition, 1997.
- [13] D.C. Groeneveld, J.Q. Shan, A.Z. Vasic, L.K.H. Leung, A. Durmayaz, J. Yang, S.C. Cheng, and A. Tanase, "The 2006 CHF look-up table", *Nuclear Engineering and Design*, **237**, pp. 1909-1922, (2007).